Supplementary Information

Direct Detection of Dimethylstannylene and Tetramethyldistannene in Solution and the Gas Phase by Laser Flash Photolysis of 1,1-Dimethylstannacyclopent-3-enes.

R. Becerra, P. P. Gaspar, C. R. Harrington, W. J. Leigh*, I. Vargas-Baca, R. Walsh*, and D. Zhou*

Spectroscopic data for 1,1-dimethyl- (4a) and 1,1,3,4-tetramethylstannacyclopent-3-ene (4b)

*1,1-Dimethyl-stannacyclopent-3-ene (**4a**).* ^{1}H NMR (C_6D_6, 300 MHz), δ = 0.10 (s, 6H, $J_{H-^{119}Sn}$ = 54.6 Hz, $SnCH_3$), 1.47 (s, 4H, $J_{H-^{119}Sn}$ = 35.1 Hz, $SnCH_2$), 6.27 (s, 2H, $J_{H-^{119}Sn}$ = 113.1 Hz, HC=CH); $^{13}C\{^{1}H\}$ NMR (C_6D_6, 75.4 MHz), δ = -10.3 ($SnCH_3$), 13.56 ($SnCH_2$), 133.03 (-CH=CH-); ^{119}Sn NMR (C_6D_6, 111.9 MHz), δ = 57.43; MS (70 eV), *m/e* (I) = 204(6), 202(6), 200(5)($M^{+\cdot}$), 189(11), 187(8), 185(6)(M^{+}-15), 165(16), 163(11), 161(9), 150(82), 148(53), 146(35), 135(100), 133(71), 131(41), 120(8), 118(7), 116(5), 54(13), 53(19); HRMS, calcd. for $C_6H_{12}{}^{120}Sn$ 203.9961; found 203.9956.

*1,1,3,4-Tetramethyl-stannacyclopent-3-ene (**4b**).* ^{1}H NMR (C_6D_6, 300 MHz), δ = 0.13 (s, 6H, $J_{H-^{119}Sn}$ = 57 Hz, $SnCH_3$), 1.59 (s, 4H, $J_{H-^{119}Sn}$ = 42 Hz, $SnCH_2$), 1.81 (s, 6H, C=C-CH_3); $^{13}C\{^{1}H\}$ NMR (C_6D_6, 75.4 MHz), δ = -11.56 ($SnCH_3$), 20.87 ($SnCH_2$, C=CCH_3), 130.91 (C=CCH_3); ^{119}Sn NMR (C_6D_6, 111.9 MHz), δ = 21.65; MS (70 ev) *m/e* (I) = 232(8), 230(7), 228(3)($M^{+\cdot}$), 217(47), 215(40), 213(19)(M^{+}-15), 165(27), 163(16), 161(12), 150(19), 148(18), 146(10), 135(100), 133(71), 131(46), 120(11), 82(15), 67(62), 65(29); HRMS, calcd. for $C_8H_{18}{}^{120}Sn$ 232.0274, found 232.0288.

Compound **4a** exhibited a (gas phase) UV absorption maximum of *ca.* 200 nm. The spectrum of **4b** in deoxygenated hexane solution at a concentration of ca 1 x 10^{-5} M showed only edge absorption between 190-225 nm.

Laser Flash Photolysis Experiments

Laser flash photolysis experiments in solution employed the pulses from a Lambda Physik Compex 120 excimer laser, filled with F_2/Ar/Ne (193 nm; 20-25 ns; *ca.* 50 mJ) mixtures, and a Luzchem Research mLFP-111 laser flash photolysis system, modified as described previously.[1] Solutions were prepared at concentrations such that the absorbance at the excitation wavelength

(193 nm) was between *ca.* 0.7 and 0.9 (3-5 x 10^{-5} M), and were flowed continuously through a thermostatted 7 x 7 mm Suprasil flow cell connected to a calibrated 100 mL reservoir; the monitoring path length of the irradiated solution was 5 mm. The solutions were deoxygenated with a stream of nitrogen gas for at least 60 minutes prior to and then throughout the duration of each experiment. Relatively rapid flow rates (ca 5 mL min^{-1}) were necessary in order to minimize fluorescence and/or light scattering and cavitation effects, presumably because of the formation of elemental tin in the photolyses. Transient decay rate constants were calculated by non-linear least squares analysis of the absorbance-time profiles, obtained by signal averaging of the data from 25-50 individual experiments, using the Prism 3.0 software package (GraphPad Software, Inc.) and the appropriate user-defined fitting equations after importing the raw data from the Luzchem mLFP software. Methanol was added directly to the reservoir by microliter syringe as aliquots of standard solutions. All errors are quoted as twice the standard deviation obtained from the least-squares analyses.

Laser flash photolysis experiments in the gas phase have been described in detail previously.[2,3] Only essential and brief details are therefore included here. The target reactive transient was produced by flash photolysis of **4a** using a Coherent Compex 100 excimer laser operating at 193 nm (ArF fill). Transient absorptions were monitored in real time by means of a Coherent Innova 90-5 argon ion laser. All 9 available lines of the probe laser were employed for spectral measurements, but for the kinetic studies the argon ion laser was generally only operated at 501.7 or 514.5 nm. Experiments were carried out in a Spectrosil quartz cell with demountable windows. The photolysis beam (4 cm x 1 cm cross-section) entered the centre of the cell laterally, while the probe beam was multi-passed longitudinally along the axis of the cell 32 or 36 times, giving a maximum absorption path length of ca 1.2 or 1.4 m, respectively. Photolysis laser pulse energies were typically 50-70 mJ with a variation of ± 5%. Light signals were measured by a dual photodiode/differential amplifier

combination, and signal decays were stored in a transient recorder (Datalab DL 910) interfaced to a BBC microcomputer. This was used to average the decays of 2 or 3 photolysis laser shots. Dust formation was a serious problem. Its effect on the decay traces was minimized by allowing time between shots for it to settle and by regular cleaning of the reaction cell.

Gas mixtures for photolysis were made up containing 10-40 mTorr of **4a**, variable pressures of reactive substrates, and with total pressures made up to 10 Torr with inert diluent (SF_6). Pressures were measured with capacitance manometers (MKS Baratron). Most measurements were carried out at room temperature (300 ± 2 K).

Steady State Photolysis Experiments

*1. Photolysis of **4a** in the gas phase.*

Preparative 193 nm photolysis of **4a** in the gas phase was carried out in a sealed Suprasil quartz cell containing the substrate (0.2 Torr) and N_2 (100 Torr) as buffer gas. Gas chromatographic analyses of reactant and product mixtures were carried out using a Perkin-Elmer 8310 chromatograph equipped with a flame ionization detector and a 3m silicone oil (OV101) column operated at 60 °C (or higher). Retention times and peak sensitivities (GC response factors) were calibrated with authentic samples.

*2. Photolysis of **4a** in hexane in the presence of trimethyltin hydride.*

A degassed hexane solution containing **4a** (0.24 M) and Me_3SnH (5 M), and a small amount of dodecane as internal standard was irradiated in a quartz tube at 254 nm in a Rayonet reactor for up to 4 hours at room temperature. The resulting photolysate was brown in color, with a bright metallic mirror deposited on the walls of the tube. The photolysis was monitored by GC/MS (HP 5890A/5971A; 30 m x 0.25 μm DB-5), allowing the detection of (only) two tin-containing products which were identified as hexamethyldistannane ($Me_3SnSnMe_3$) and pentamethyldistannane ($Me_3SnSnMe_2H$) on the basis of their mass spectra (Figure 3S); the latter

exhibited the shorter retention time, as indicated on the spectra. The spectrum of the former is in good agreement with that reported by Lappert and coworkers.[4]

The product yields reported in eq 2 of the article were obtained by GC/MS analysis of degassed hexane solutions containing 0.17 M Me_3SnH, a small amount of dodecane, and 0 or 0.08 M **4a**, which were irradiated in parallel in quartz tubes at room temperature for 3 hours.

*3. Photolysis of **4b** in cyclohexane-d_{12} in the presence of MeOH.*

Deoxygenated 0.02 M solutions of **4b** in cyclohexane-d_{12}, one containing 0.5 M MeOH and one not, were irradiated with the light from a Philips 93106E Zn resonance lamp (214 nm), with periodic monitoring of the photolysate by (600 MHz) ^{1}H NMR spectroscopy. The spectra of the two solutions after an irradiation period of 2.5 hours are shown in Figure 4S. Resonances due to **4b** appear at δ 0.21 (6H), 1.57 (4H), and 1.72 (6H), while those due to 2,3-dimethyl-1,3-butadiene (DMB) appear at δ 1.89 (6H), 4.91 (2H), and 5.01 (2H). The multiplets at δ 0.89, 0.97, and 1.30 are due to hydrocarbon impurities in the sample of **4b** used for the experiment, while that at δ 1.38 is due to residual solvent protons (i.e. $C_6D_{11}H$) and served as the internal integration standard.

Computational details. *Molecular structures.* Calculations were performed with the ADF 2003.01 or 2004.01 density functional theory package (SCM).[5-7] The calculation of model geometries was gradient-corrected with the exchange and correlation functionals of Perdew and Wang (PW91);[8] all basis functions were of triple-ζ quality and were composed of uncontracted Slater-type orbitals (STOs), including all core electrons and two auxiliary basis sets of STOs for polarization. Zero-order relativistic corrections (the ZORA formalism) were applied for all calculations of Sn-containing species. The homolytic dissociation energy of Sn_2Me_6 was calculated as the difference of total bonding energy of the fully optimized molecule and the

average-of-configuration bonding energy of the $SnMe_3$ radical optimized at the unrestricted level, the number is not corrected for zero-point energy.

Spectroscopic calculations. The method is based on the time-dependent extension of density functional theory (TD-DFT) implemented[9-13] in the ADF package. The Adiabatic Local Density Approximation (ALDA) was used for the exchange-correlation kernel[14,15] and the differentiated static LDA expression was used with the Vosko-Wilk-Nusair parametrization.[16] Zero-order relativistic corrections (ZORA) were applied in all cases. For the exchange-correlation potentials in the zeroth-order KS equations, the first ten excitation energies and oscillator strengths were obtained using the Davidson iterative diagonalization method.

Table 1S. Comparison of experimental and calculated structural data for **9**.

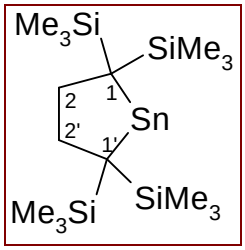

Distances (Å)	Experimental [a]	DFT (PW91/TZ2P/ZORA)
Sn-C	2.218 (7)	2.254
	2.223 (7)	2.254
C1-C2	1.583 (10)	1.562
C2-C2'	1.482 (10)	1.545
Si1-C1	1.869 (7)	1.913
Si2-C1	1.898 (7)	1.905
Si1-C(Me)	1.887 (12)	1.899-1.903
Angles (°)		
C1-Sn-C1	86.7 (2)	85.7
C1-Si-C(Me)	110.0 (4)	111.6
C(Me)-Si-C(Me)	104.5 (4)	104.7
Sn-C1-C2	103.7 (4)	104.3
Sn-C1-Si1	102.0 (3)	101.9
C1-C2-C2'	113.5 (6)	113.9
C2-C2'-C1'	115.8 (6)	113.9

[a] Reference [17].

Table 2S. Calculated Sn-centered molecular dimensions of $SnMe_2$ and $(SnMe_2)_n$ oligomers (n=2-4).

	$SnMe_2$	$Me_2Sn=SnMe_2$ (**5b**)		*cyclo*-Sn_3Me_6 (**7**)	*cyclo*-Sn_4Me_8 (**8**)
		C_i symmetry	No symmetry [a]		
r_{Sn-C} (Å)	2.218	2.203	2.203,2.204	2.19	2.19
r_{Sn-Sn} (Å)	–	2.778	2.772	2.87 - 2.88	2.87
$\angle_{C-Sn-C}$ (^{o})	92.7	101.9	100.9, 101.1	109.6 - 109.8	106.6
$\angle_{Sn-Sn-C}$ (^{o})	–	114.5, 114.6	113.3,116.2,113.3,116.1	119.3 - 119.9	110.4, 120.9
$\angle_{Sn-Sn-Sn}$ (^{o})	–	–	–	60	86.5
Fold angle (β, ^{o})	–	48.80	48.74	–	39.63

[a] The structure is twisted about the Sn=Sn bond by an angle θ =11.78^o.

Table 3S. Comparison of experimental and calculated UV-vis spectra of stannylene **9**.

Calculated				Experimental [a]			
Sym.	ΔE (eV)	λ_{max} (nm)	f	ΔE (eV)	λ_{max} (nm)	ε ($M^{-1}cm^{-1}$)	$\Delta\Delta$E (eV)
1B	**2.456**	**505**	**3.69E-03**	**2.56**	**484**	**400**	**0.10**
1A	2.934	423	3.66E-05				
2B	3.581	346	1.57E-02	3.35	370	90	0.23
2A	3.923	316	3.11E-03				
3B	4.370	284	3.34E-04				
3A	4.375	283	2.41E-04				
4A	4.410	281	1.04E-02	4.35	285	770	0.02
4B	4.486	276	4.93E-03				
5B	4.569	271	1.64E-02				
6B	4.577	271	9.728E-02	5.02	247	9700	0.53

[a] Reference [17].

Tables 4S. Calculated energies and oscillator strengths (ℓ) of the first 10 allowed transitions of $SnMe_2$, $(SnMe_2)$-oligomers (**5b**, **7**, and **8**), $SiMe_2$, and Si_2Me_4 (**11b**).

$SnMe_2$ (C_2 symmetry)				Sn_2Me_4 (**5b**; C_i symmetry)				Sn_2Me_4 (**5b**; no symmetry)			
Sym.	ΔE(eV)	λ_{max}(nm)	ℓ	Sym.	ΔE(eV)	λ_{max}(nm)	ℓ	Sym.	ΔE(eV)	λ_{max}(nm)	ℓ
1B	2.473	501	1.82E-02	$1A_u$	2.79	444	2.58E-01	1A	2.78	447	2.52E-01
1A	3.392	365	5.80E-05	$2A_u$	3.97	312	6.51E-03	2A	3.34	372	7.99E-05
2B	5.174	240	2.00E-01	$3A_u$	4.65	267	1.13E-03	3A	3.64	341	3.53E-03
2A	5.200	238	6.32E-02	$4A_u$	5.25	236	6.22E-03	4A	3.93	315	3.69E-03
3A	6.044	205	7.35E-02	$5A_u$	5.50	225	8.59E-02	5A	3.97	312	1.70E-04
4A	6.319	196	2.67E-01	$6A_u$	5.51	225	8.83E-02	6A	3.98	311	3.20E-03
3B	6.326	196	8.10E-02	$7A_u$	5.66	219	6.21E-02	7A	4.67	266	2.06E-03
5A	6.352	195	3.05E-02	$8A_u$	5.93	209	3.25E-01	8A	4.84	256	9.74E-06
4B	6.524	190	3.34E-02	$9A_u$	5.96	208	2.51E-01	9A	5.30	234	2.11E-03
5B	6.560	189	4.07E-02	$10A_u$	6.04	205	6.21E-02	10A	5.50	225	6.31E-02

Sn_3Me_6 (**7**; no symmetry)				Sn_4Me_8 (**8**; D_{2d} symmetry)			
Sym.	ΔE(eV)	λ_{max}(nm)	ℓ	Sym.	ΔE(eV)	λ_{max}(nm)	ℓ
1A	3.36	369	1.28E-06	1E	4.02	308	2.17E-02
2A	3.37	368	7.97E-07	2E	4.22	294	2.06E-01
3A	3.58	346	3.19E-06	3E	4.39	282	2.05E-02
4A	3.72	333	1.34E-04	4E	4.54	273	4.35E-02
5A	3.85	322	1.86E-02	5E	4.72	263	1.54E-01
6A	3.86	321	1.86E-02	$1B_2$	4.74	261	3.23E-04
7A	4.16	298	2.23E-01	6E	4.97	249	2.38E-01
8A	4.17	297	2.26E-01	$2B_2$	4.97	249	5.90E-05
9A	5.96	208	1.38E-00	7E	5.19	239	2.96E-01
10A	5.97	208	1.39E-00	$3B_2$	5.27	235	4.64E-02

$SiMe_2$ (C_2 symmetry)				Si_2Me_4 (**11b**; C_i symmetry)			
Sym.	ΔE(eV)	λ_{max}(nm)	ℓ	Sym.	ΔE(eV)	λ_{max}(nm)	ℓ
1B	2.71	457	2.31E-02	$1A_u$	3.39	365	1.91E-01
1A	4.59	270	1.89E-04	$2A_u$	4.31	287	1.30E-01
2A	5.05	245	4.49E-02	$3A_u$	5.34	232	1.09E-02
2B	5.34	232	1.95E-01	$4A_u$	5.37	231	1.65E-02
3B	6.23	199	7.20E-02	$5A_u$	5.55	224	7.34E-03
3A	6.25	199	2.47E-01	$6A_u$	5.94	209	5.12E-02
4A	6.50	191	1.62E-02	$7A_u$	6.12	203	4.59E-04
5A	6.83	181	1.03E-01	$8A_u$	6.25	198	1.57E-01
4B	6.94	179	9.38E-03	$9A_u$	6.67	186	1.82E-01
6A	6.96	178	4.03E-04	$10A_u$	6.74	184	1.48E-01

Table 5S. Calculated structural parameters and Kohn-Sham energies (PW91) of the highest occupied molecular orbitals (-E_{HOMO}) for metallylenes and dimetallenes. [a]

	M = Si			**M = Ge**			**M = Sn**		
	R = H	R = CH_3	R = C_6H_5	R = H	R = CH_3	R = C_6H_5	R = H	R = CH_3	R = C_6H_5
Metallylenes									
$r_{M\text{-}R}$ (Å)	1.535	1.911	1.897	1.606	2.015	1.993	1.788	2.218	2.203
$\angle_{R\text{-}M\text{-}R}$ (^{o})	90.3	97.9	99.6	89.90	97.10	98.70	89.90	92.7	96.1
E_{HOMO} (eV)	-5.93	-4.97	-5.03	-6.03	-5.11	-5.22	-5.75	-5.03	-5.18
Dimetallenes (C_i symmetry)									
$r_{M\text{-}M}$ (Å)	2.181	2.202	2.189	2.297	2.333	2.327	2.708	2.778	2.772
$r_{M\text{-}R}$ (Å)	1.490	1.898	1.869,1.880	1.549	1.994	1.972,1.977	1.742	2.203	2.179,2.191
$\angle_{R\text{-}M\text{-}R}$ (^{o})	112.6	110.4	109.7	108.2	108.30	106.9	102.9	101.9	103.0
$\angle_{M\text{-}M\text{-}R}$ (^{o})	118.7	119.2	120.0,121.7	115.5	116.50,116.20	117.4,120.9	113.3,113.5	114.5,114.6	113.2,113.7
β (^{o})	30.07	31.11	26.94	42.84	40.17	35.01	50.37	48.80	50.22
E_{HOMO} (eV)	-5.46	-4.23	-4.43	-5.62	-4.45	-4.66	-5.50	-4.57	-4.79

[a] Calculations for stannylenes and distannenes include relativistic corrections (ZORA formalism).

Estimation of the rate constant for $SnMe_2$ recombination in the gas phase

The rate constant required to give a ca 10% yield of dimer (**5b**) in the gas phase laser flash photolysis experiments can be approximately estimated as follows. From the experimental conditions (% absorption, path length) and an assumed extinction coefficient of 1000 $dm^3\ mol^{-1}\ cm^{-1}$, an initial concentration of $SnMe_2$ of 2.0×10^{14} molecule cm^{-3} (~ 0.33 μM) in a typical experiment can be estimated. This would give rise to a final concentration of ca 1.0×10^{13} molecule cm^{-3} (~ 1.7×10^{-8} M) of **5b** if the latter is formed in 10% yield. The effective second order rate constant, k_{rec}, can be calculated from equation (1), where k_{dec} is the decay constant for the dominant first order loss process and $[SnMe_2]_o$ and $[\mathbf{5b}]_f$ are the initial and final concentrations, respectively (see next section for derivation). Using the mean observed value of $k_{dec} = 5.5 \times 10^4\ s^{-1}$ yields a value for $k_{rec} = 8 \times 10^9\ M^{-1}\ s^{-1}$. This value is in good agreement with the solution value (~$7 \times 10^9\ M^{-1}\ s^{-1}$) obtained in the solution phase experiments and is about a factor of 20 less than the collision rate. It is, in fact, typical for a radical recombination process.[18]

$$k_{rec}[SnMe_2]_o^2 = k_{dec}\,[\mathbf{5b}]_f \qquad (1)$$

Because gas-phase radical recombination processes can be pressure dependent,[18] a check was made using RRKM theory[19] as to whether the $SnMe_2$ recombination rate constant (k_{rec}) might be below its high pressure limit, k_{rec}^{∞}. The pressure dependence calculation is based on that for the reverse decomposition of Sn_2Me_4.[19] The required parameters for this calculation are shown in Table 6S. The vibrational wavenumbers for the molecule were based on typical group values and those for the transition state (TS1) were estimated to correspond to a loose structure with an *A* factor of $10^{16.5}\ s^{-1}$. Critical energies (E_o) were investigated in the range 20-30 kcal mol^{-1} corresponding to the TD-DFT value calculated in this work. A weak collision (stepladder) model

with $\langle\Delta E\rangle_{down}$ = 1000 cm^{-1} was employed. Derived values for k_{rec}/k_{rec}^{∞} are shown in Table 7S. The key values for this study pertain to P = 10 Torr and therefore lie in the range 0.98 – 0.55, with 0.88 corresponding to E_o = 25 kcal mol^{-1}. A looser transition state (TS2, $A = 10^{17.0}$ s^{-1}) was also briefly explored. With E_o = 25 kcal mol^{-1}, k_{rec}/k_{rec}^{∞} was calculated to be 0.78 at 10 Torr (SF_6).

Equation 1 (above) was derived from the rate equation for competitive 1st and 2nd order decay processes:

$$\begin{aligned} R &\rightarrow P_1 \qquad k_{dec} \\ 2R &\rightarrow P_2 \qquad k_{rec} \end{aligned}$$

$$\text{Rate} = -\frac{d[R]}{dt} = k_{dec}[R] + 2k_{rec}[R]^2$$

Assuming the first term is dominant. $\qquad [R] = [R]_0 \exp(-k_{dec}t)$

To obtain yield of P_2, viz $[P_2]_f$, requires integration

$$\frac{d[P_2]}{dt} = 2k_{rec}[R]^2 = 2k_{rec}[R]_0^2(\exp(-k_{dec}t))^2$$

$$\therefore [P_2]_f = 2k_{rec}[R]_0^2 \int_0^{\infty} \exp(-2k_{dec}t)dt$$

$$= 2k_{rec}[R]_o^2 \frac{1}{2k_{dec}} \left[\exp(-2k_{dec}t\right]_{\infty}^{0}$$

$$= 2k_{rec}[R]_0^2 \frac{1}{2k_{dec}}[1-0]$$

$$\therefore k_{rec}[R]_o^2 = k_{dec}[P_2]_f$$

Table 6S. Molecular and transition state parameters for RRKM calculation for Sn_2Me_4 decomposition (and $SnMe_2$ combination).

parameter	Sn_2Me_4	TS1
$\tilde{\nu} / cm^{-1}$	2980(8)	2980(8)
	2950(2)	2950(2)
	2900(2)	2900(2)
	1470(8)	1470(8)
	1385(4)	1385(4)
	1000(4)	1000(4)
	700(4)	700(4)
	510(4)	510(4)
	250(2)	250(2)
	210(1)	rxn coord
	190(4)	31(4)
	90(4)	90(4)
	65(1)	15(1)
A/s^{-1}		3.2×10^{16}
E_o/kcal mol^{-1}		25.0
$Z/10^{-10}$ cm^3 molecule^{-1} s^{-1} [a]		4.35

[a] Collision number for TS1..SF_6 collisions

Table 7S. Calculated RRKM pressure dependence (k_{rec}/k_{rec}^{∞}) for Sn_2Me_4 decomposition[a] (and $SnMe_2$ combination) in SF_6 bath gas at various critical energies (E_o).

P/Torr	10^4	10^3	10^2	30	10	3	1	0.1
30[b]	1.00	1.00	1.00	0.99	0.98	0.95	0.91	0.71
25[b]	1.00	1.00	0.98	0.94	0.88	0.78	0.65	0.36
20[b]	1.00	0.96	0.82	0.69	0.55	0.38	0.26	0.086

[a] log (A/s^{-1}) = 16.5 [b] E_o values (kcal mol^{-1})

Figure 1S. Transient decay profiles recorded at 430, 540, and 560 nm. The solid lines in the individual traces are the non-linear least squares fits of the data to second order decay kinetics.

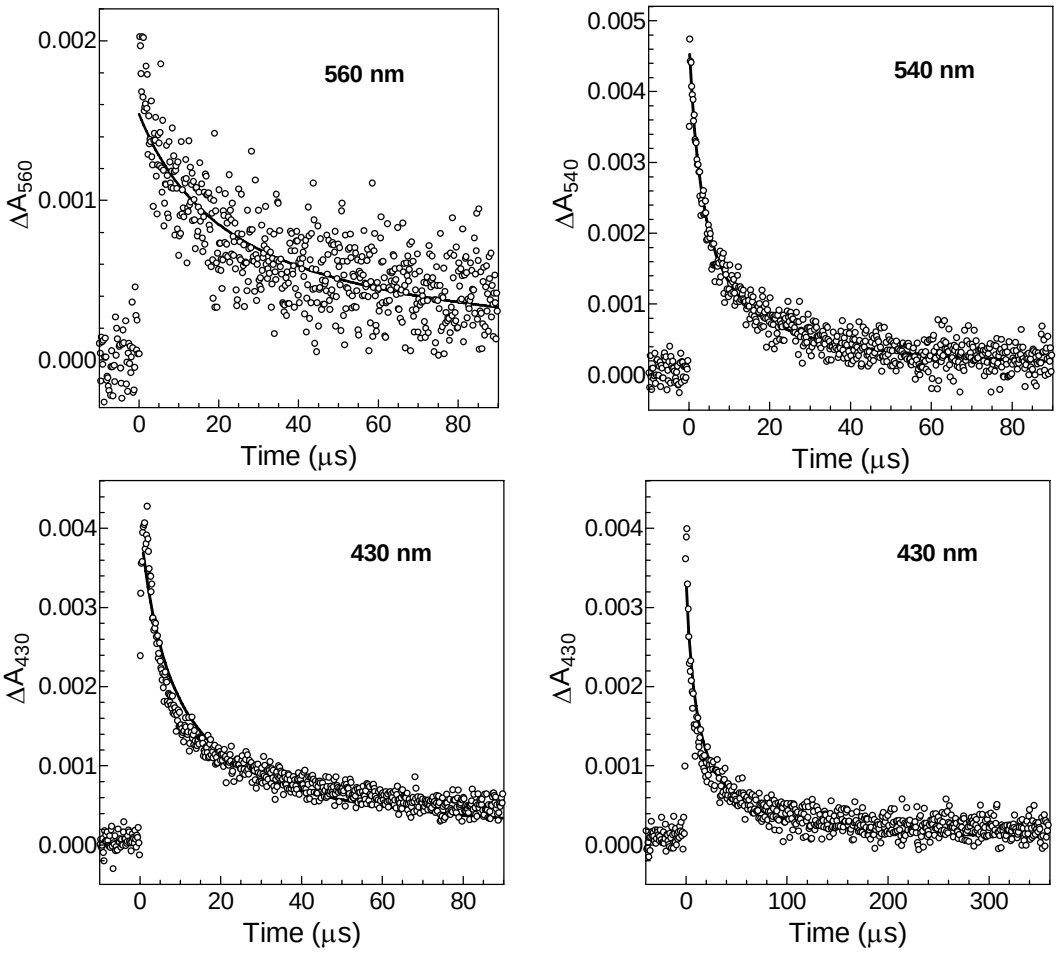

Figure 2S. Transient decay profiles recorded at (a) 530 nm and (b) 440 nm in the presence of 0, 0.5, and 1.0 mM MeOH, by laser flash photolysis of a deoxygenated solution of **4b** in hexane at 25 °C.

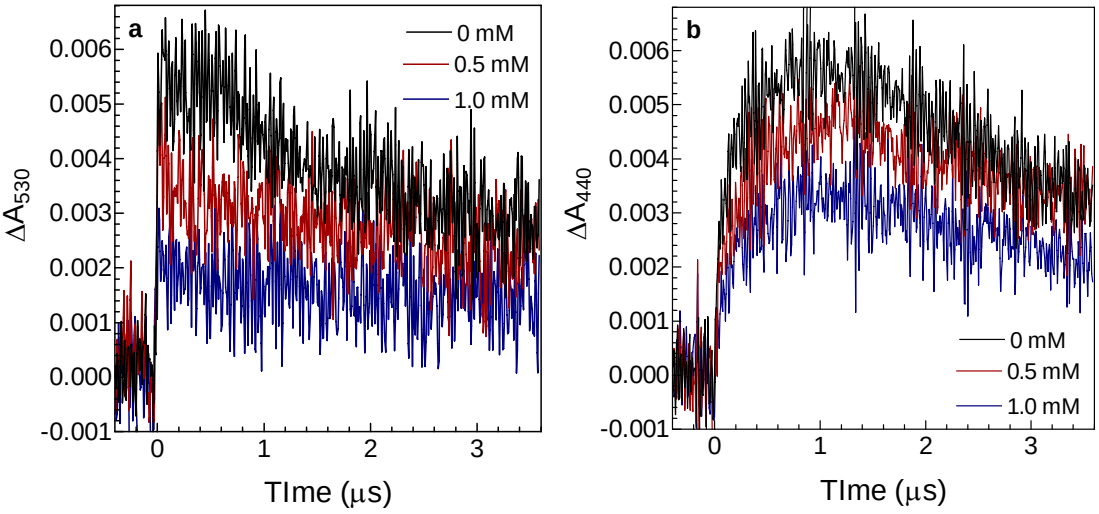

Figure 3S. (a) Mass spectrum of hexamethyldistannane, recorded by GC/MS analysis of the mixture obtained from photolysis of a 0.5 M solution of **4a** in hexane containing 5.0 M Me_3SnH.

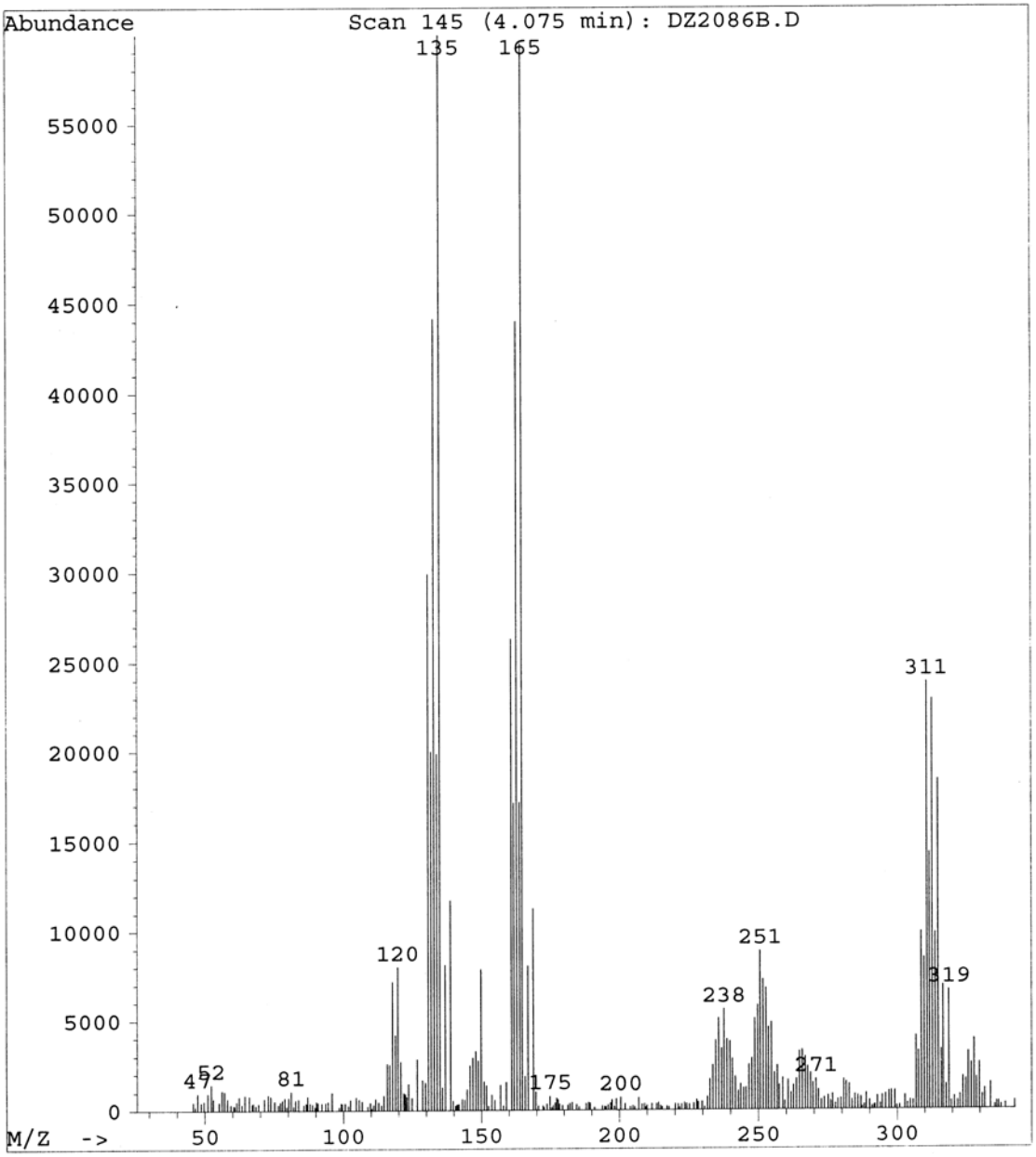

Figure 3S. (b) Mass spectrum of pentamethyldistannane, recorded by GC/MS analysis of the mixture obtained from photolysis of a 0.5 M solution of **4a** in hexane containing 5.0 M Me_3SnH.

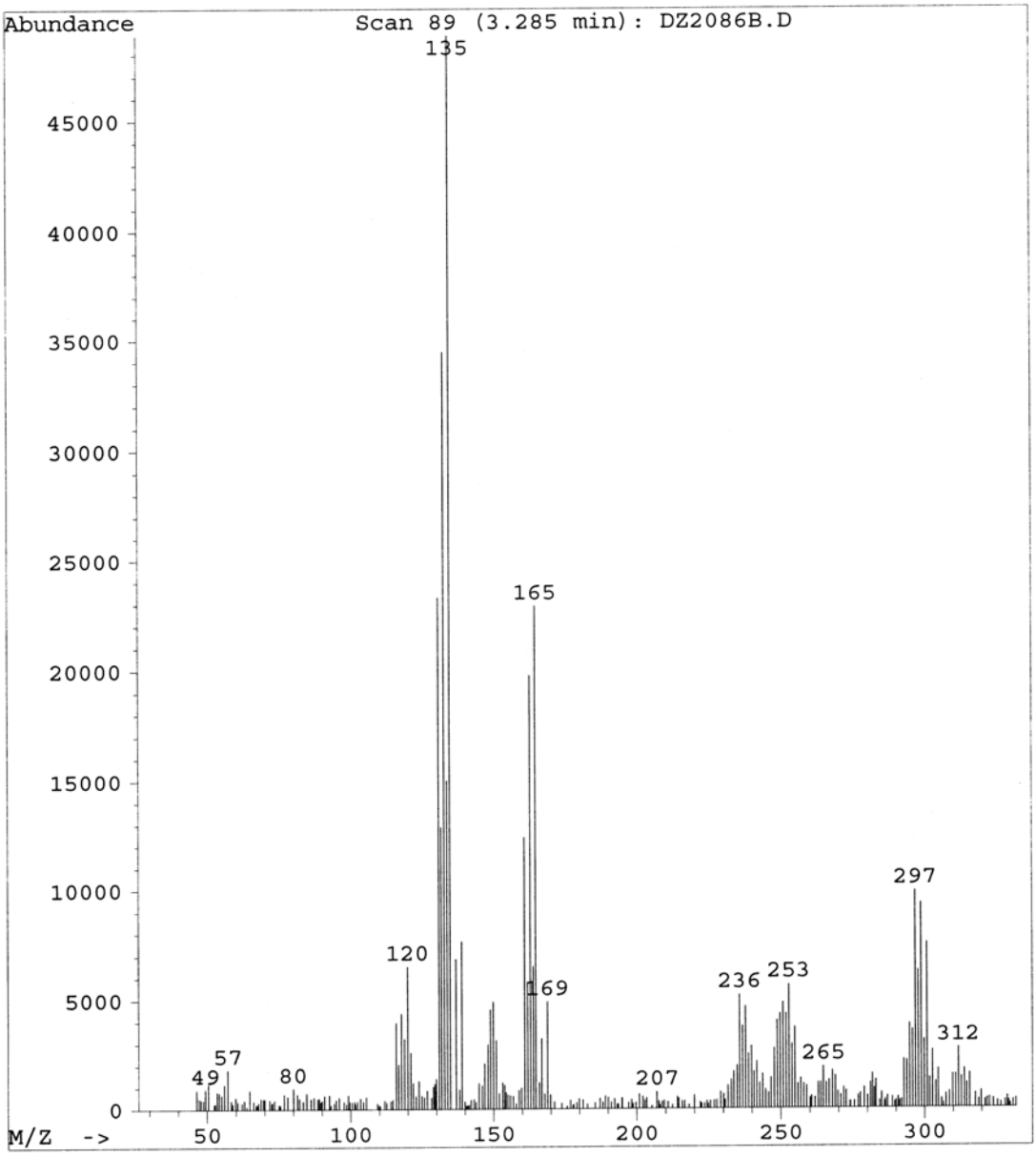

Figure 4S. 600 MHz ^{1}H NMR spectra of deoxygenated solutions of **4b** (0.02 M) in cyclohexane-d_{12} containing (a) 0 M and (b) 0.5 M MeOH, after irradiation with 214 nm light for 2.5 hours.

(a)

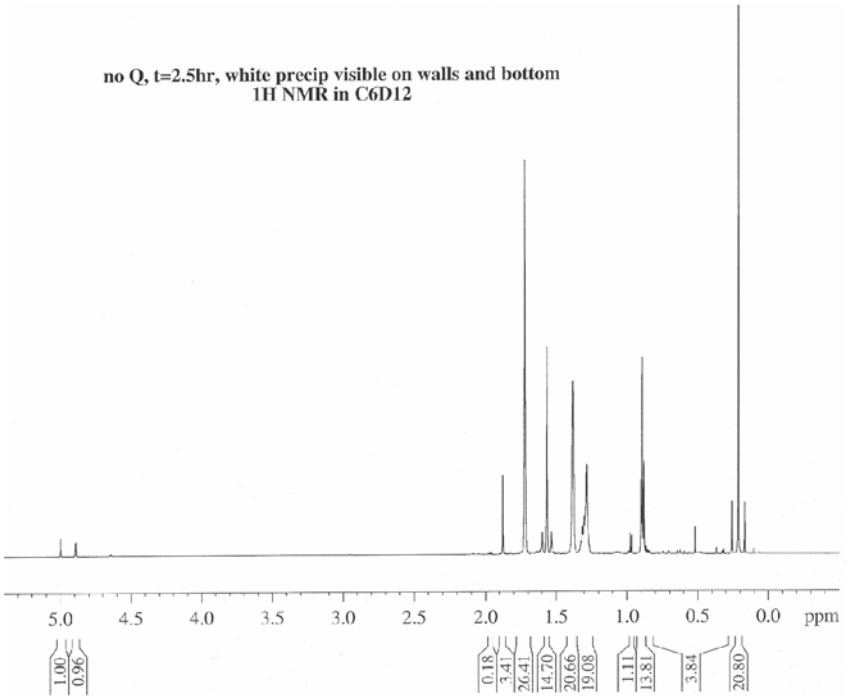

(b)

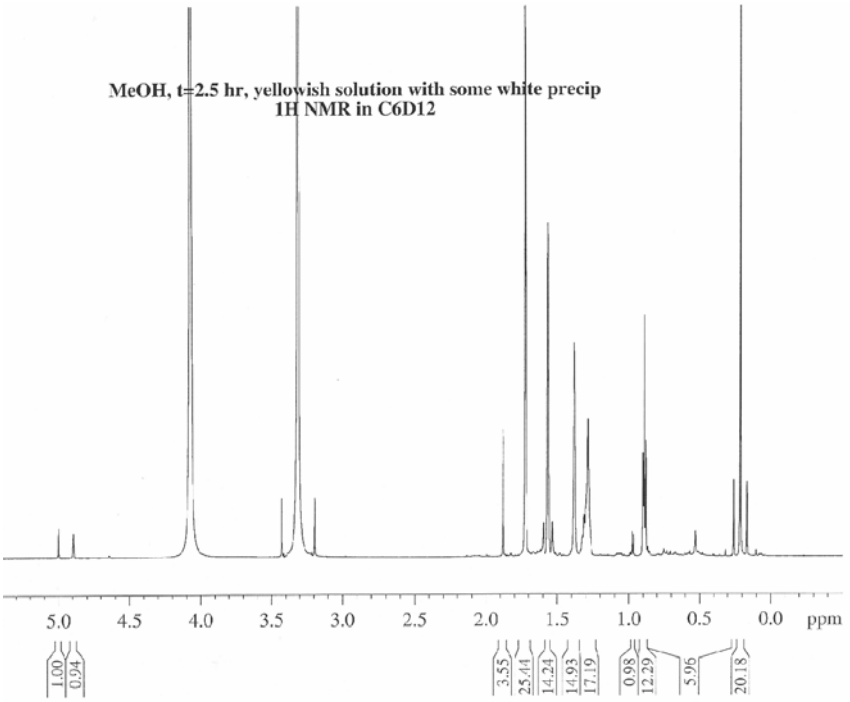

References

(1) Leigh, W. J.; Harrington, C. R.; Vargas-Baca, I. *J. Am. Chem. Soc.* **2004**, *126*, 16105.

(2) Becerra, R.; Boganov, S. E.; Egorov, M. P.; Lee, V. Ya.; Nefedov, O. M.; Walsh, R. *Chem. Phys. Lett.* **1996**, *250*, 111.

(3) Becerra, R.; Boganov, S. E.; Egorov, M. P.; Faustov, V. I.; Krylova, I. V.; Nefedov, O. M.; Walsh, R. *J. Am. Chem. Soc.* **2002**, *124*, 7555.

(4) Lappert, M. F.; Pedley, J. B.; Simpson, J.; Spalding, T. R. *J. Organomet. Chem.* **1971**, *29*, 195.

(5) te Velde, G.; Bickelhaupt, F. M.; van Gisbergen, S. J. A.; Fonseca Guerra, C.; Baerends, E. J.; Snijders, J. G.; Ziegler, T. *J. Comput. Chem.* **2001**, *22*, 931.

(6) Fonseca Guerra, C.; Snijders, J. G.; te Velde, G.; Baerends, E. J. *Theor. Chem. Acc.* **1998**, *99*, 391.

(7) Baerends, E. J., Autschbach, J., Berces, A., Bo, C., Boerrigter, P. M., Cavallo, L., Chong, D. P., Deng, L., Dickson, R. M., Ellis, D. E., Fan, L., Fischer, T. H., Fonseca Guerra, C., van Gisbergen, S. J. A., Groeneveld, J. A., Gritsenko, O. V., Gruning, M., Harris, F. E., van den Hoek, P., Jacobsen, H., van Kessel, G., Kootstra, F., van Lenthe, E., Osinga, V. P., Patchkovskii, S., Philipsen, P. H. T., Post, D., Pye, C. C., Ravenek, W., Ros, P., Schipper, P. R. T., Schreckenbach, G., Snijders, J. G., Sola, M., Swart, M., Swerhone, D., te Velde, G., Vernooijs, P., Versluis, L., Visser, O., van Wezenbeek, E., Wiesenekker, G., Wolff, S. K., Woo, T. K., and Ziegler, T. ADF2003.01. 2003.01. 2002. Amsterdam, SCM.

(8) Perdew, J. P.; Chevary, J. A.; Vosko, S. H.; Jackson, K. A.; Pederson, M. R.; Singh, D. J.; Fiolhais, C. *Phys. Rev. B* **1992**, *46*, 6671.

(9) Gross, E. K. U.; Kohn, W. *Adv. Quantum Chem.* **1990**, *21*, 255.

(10) Gross, E. K. U.; Ullrich, C. A.; Gossmann, U. J. *Density functional theory of time-dependent systems*; Plenum: New York, 1995; p 149.

(11) Gross, E. K. U.; Dobson, J. F.; Petersilka, M. *Density Functional Theory*; Springer: Heidelberg, 1996.

(12) van Gisbergen, S. J. A.; Snijders, J. G.; Baerends, E. J. *J. Chem. Phys.* **1995**, *103*, 9347.

(13) van Gisbergen, S. J. A.; Snijders, J. G.; Baerends, E. J. *Comput. Phys. Commun.* **1999**, *118*, 119.

(14) van Gisbergen, S. J. A.; Snijders, J. G.; Baerends, E. J. *Phys. Rev. Lett.* **1997**, *78*, 3097.

(15) van Gisbergen, S. J. A.; Snijders, J. G.; Baerends, E. J. *J. Chem. Phys.* **1998**, *109*, 10644.

(16) Vosko, S. H.; Wilk, L.; Nusair, M. *Can. J. Phys.* **1980**, *58*, 1200.

(17) Kira, M.; Yauchibara, R.; Hirano, R.; Kabuto, C.; Sakurai, H. *J. Am. Chem. Soc.* **1991**, *113*, 7785.

(18) Davies, J. W.; Pilling, M. J. In *Adv. Gas Phase Photochem. Kinetics, Vol. 2*; Ashfold, M. N. R., Baggott, J. E., eds. Royal Society of Chemistry: London, 1989; pp 105-170.

(19) Holbrook, K. A.; Pilling, M. J.; Robertson, S. H. *Unimolecular Reactions*; John Wiley and Sons: Chichester, 1996.